Journal of Computer Assisted Tomography
8(4):594–598, August

NMR Even Echo Rephasing in Slow Laminar Flow

Victor Waluch and William G. Bradley

Abstract: In nuclear magnetic resonance (NMR) imaging, flowing fluids possess several unusual properties not found in stationary materials. One of these is the strong signal emitted during slow flow by unsaturated protons just entering the imaging volume. Another is the observation that even echoes of a multiple spin-echo train have higher intensity than the odd. The two phenomena have not previously been distinguished in the NMR imaging literature and the term "paradoxical enhancement" has been applied to both. In this communication we consider the conditions under which such a phenomenon occurs, derive general mathematical relationships, and show clinical examples in which an understanding of spin-echo rephasing is especially useful. **Index Terms:** Nuclear magnetic resonance, techniques—Blood, flow dynamics—Nuclear magnetic resonance.

The intensity (I) of the spin-echo signal in nuclear magnetic resonance (NMR) depends on four variables: proton density N(H), the two magnetic relaxation times T1 and T2, and a flow function f(v). Dependence on mobile proton density is linear and dependence on the relaxation times is first-order exponential:

$$I = N(H)f(v)e^{-TE/T2}(1 - e^{-TR/T1}), \qquad (1)$$

where TR is the repetition time and TE is the echo delay time, which are under computer control. This article discusses the flow function f(v) in slow laminar flow.

During clinical NMR imaging we have frequently noted a stronger signal coming from veins on the second spin echo (TE = 56 ms) than on the first (TE = 28 ms). We believe this represents a rephasing phenomenon that is only seen on even echoes during slow laminar flow. This article discusses this phenomenon and derives the pertinent equations.

When discussing blood flow, one must consider the velocity (speed and direction of flow), the diameter of the vessel, the density and viscosity of blood, and whether the flow is pulsatile or steady. If the flow is steady, knowledge of the above parameters allows one to calculate the Reynolds number Re (Re = vessel diameter × velocity × density/viscosity). If Re is less than 2,100, flow is generally laminar; if greater than 2,100, it is generally turbulent (1). Finally, blood flow must be considered in the context of the specific pulsing sequence.

When multiple repetitions are taken, slow flow of unsaturated protons into the imaging volume increases signal strength relative to the adjacent, partially saturated stationary tissue. This has been called "flow related enhancement" (2).

If flow is rapid, some downstream protons leave the imaging volume prior to exposure to all radiofrequency (RF) pulses in the sequence and consequently do not contribute to the signal. Also, upstream protons enter the imaging volume after the 90° pulse and therefore will not give a spin echo. For both reasons, the NMR intensity decreases. This has been called "high velocity signal loss" (2).

This paper addresses only slow laminar flow and specifically focuses on even echoes in the Carl-Purcell-Meiboom-Gill echo train. The problem can be stated as follows: if the intensities of the first and second echoes are considered, the second echo should be less intense than the first because of T2 relaxation. However, in slow laminar flow the ob-

From the NMR Imaging Laboratory, Huntington Medical Research Institutes, and Department of Radiology, Huntington Memorial Hospital, Pasadena, CA (W. G. Bradley). (Dr. Waluch is a Diasonics NMR fellow.) Address correspondence and reprint requests to Dr. Bradley at NMR Imaging Laboratory, Huntington Medical Research Institutes, 18 Pico Street, Pasadena, CA 91105.

served signal from the second echo is often much greater than the first. Qualitatively, this is due to incomplete rephasing following the first 180° RF pulse, which decreases the intensity of the first spin echo. Following an additional 180° of rotation, rephasing is complete, producing a more intense second echo.

To appreciate this phenomenon quantitatively requires an understanding of "isochromats," which have been defined as hypothetically small groups of protons that precess in phase throughout the spin-echo sequence (3–5). These isochromats gain phase according to the Larmor expression relating the local magnetic field H and the gyromagnetic ratio γ:

$$f = \gamma * H \tag{2}$$

$$d\phi = \gamma * H * dt \tag{3}$$

where f is the frequency and $d\phi$ is the differential phase measured in units of 2π radians accumulated in differential time dt.

If the local magnetic field H is constant in space, the isochromats all gain phase at the same rate and no phase difference develops. At time t all isochromats have the same phase:

$$\phi = \gamma * H * t \tag{4}$$

However, since there are nonuniformities in the external magnetic field as well as in the local magnetic environment of the isochromats, a phase difference develops between the different isochromats. If the nonuniformities are not too severe, the usual spin-echo techniques cause a rephasing of the isochromats at the time of the spin echo. This is done by applying a 180° pulse, which reverses the sign of the developed phase at time $t = \tau$ for each isochromat. Since the isochromats continue to precess in the same direction, they will rephase at a time $2*\tau$.

The spin phase graph (5) is useful in understanding this (Fig. 1). In Fig. 1 curves a through c represent three isochromats. Curve a gains phase relative to the master oscillator and curve c looses phase relative to the oscillator. Curve b remains in phase with the oscillator. At 15 ms (t = TE/2) the phases are reversed by a 180° pulse, which rotates the local magnetization vectors. The isochromats rephase at all spin echoes. This discussion applies as long as there are no magnetic field gradients or the isochromats are stationary.

When gradient fields are present, the situation is somewhat more complicated. Consider the direction of both flow and a linear gradient, g, to be along the z axis of the main magnetic field. The net magnetic field is then given by

$$H(z) = H_0 + g*z. \tag{5}$$

Initially, the isochromats in various lamina are in phase but soon diverge as in Fig. 1. However, the

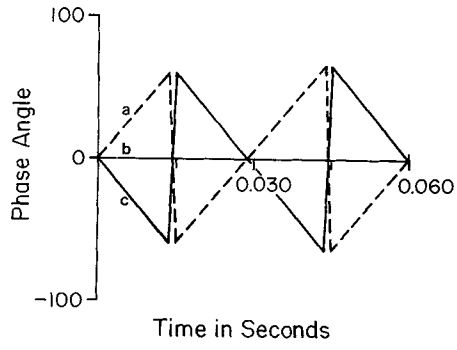

FIG. 1. Phase graph. Stationary materials in different values of magnetic field. As a function of time, curve a shows phase gain, curve c shows phase lag, curve b shows no phase change.

phase growth curves are not linear but quadratic as follows:

$$d\phi = \gamma * H(z) * dt \tag{6}$$

$$d\phi = \gamma * H_0 * dt + \gamma * g * z * dt \tag{7}$$

At time t the position z of each isochromat will depend on its velocity v as given by $z = v*t$. Thus,

$$d\phi = \gamma * H_0 * dt + \gamma * g * v * t * dt \tag{8}$$

$$\phi = \gamma * H_0 * t + \gamma * g * v * t^2/2 + C, \tag{9}$$

where it is to be understood that v may differ for each isochromat and C is a constant of integration. The expression for phase is derived as a function of time when the phase is reversed at times $1*\tau$, $3*\tau$, $5*\tau$, etc. Let j indicate the jth phase inversion. Let $k = \gamma\, gv/2$, then the phase as a function of time t after the jth phase inversion and before the jth + 1 inversion is given by the recursive expressions:

$$F_j(t) = k*t^2 - k*[(2*j - 1)*\tau]^2 - F_{j-1}[(2*j - 1)*\tau] \tag{10}$$

$$f_j(t) = \gamma * H_0 * t - f_{j-1}[2(2j - 1)*\tau] \tag{11}$$

where $F_{-1} = -k*\tau^2$ and $f_{-1} = 0$.

In the above expression the quadratic and the linear phase terms have been separated into F and f, respectively. Total phase is given by the sum of F_j and f_j. In Table 1 several of these terms are eval-

TABLE 1. *Quadratic (F) and linear (f) phase terms in the case of linear gradients*

j	$F_j/{}^1/_2\gamma gv$	$f_j/\gamma H_0$
1	$t^2 - 2*\tau^2$	$(t - 2*\tau)$
2	$t^2 - 16*\tau^2$	$(t - 4*\tau)$
3	$t^2 - 34*\tau^2$	$(t - 6*\tau)$
4	$t^2 - 64*\tau^2$	$(t - 8*\tau)$
5	$t^2 - 98*\tau^2$	$(t - 10*\tau)$
6	$t^2 - 144*\tau^2$	$(t - 12*\tau)$
7	$t^2 - 194*\tau^2$	$(t - 14*\tau)$

uated. These recursive expressions can be solved for a general field gradient by means of some tedious algebra from which the reader is spared (6). If it is assumed that the gradient is expandable in a Taylor power series, the nth power term in the phase expression (corresponding to the $n-1$st term in the gradient expansion) is given by

$$\Phi_j^n/k = t^n + (-1)^j * 2^* \tau^n \sum_{i=0}^{j-1} (-1)^i (2i + 1)^n \quad (12)$$

where for $n = 1$, $k = \gamma H_0$; for $n = 2$, $k = \gamma * g * v/2$; and for n > 2, k = appropriate factors.

DISCUSSION

Consider the case of a uniform field where the phase grows as the first power of time, i.e., $n = 1$. This is the case of stationary materials even in the presence of field gradients. Only the $n = 1$ term of Eq. 12 is present; the higher terms being identically zero. After the first inversion ($j = 1$), at $t = \tau$

$$\Phi_1^1 = (t - 2^*\tau)^*\gamma^* H_0 \quad (13)$$

which at the first echo ($t = 2^*\tau$) becomes

$$\Phi_1^1 = (2^*\tau - 2^*\tau)^*\gamma^* H_0 = 0. \quad (14)$$

At the second echo ($j = 2$, $t = 4^*\tau$),

$$\Phi_2^1 = [t - 2^*\tau^*(1 - 3)] = (4^*\tau - 2^*\tau^* 2) = 0 \quad (15)$$

which as may be seen is zero at $t = 4^*\tau$. This shows that rephasing of isochromats is exact at both the odd and even echoes in the case of no field gradients or no flow.

In the case of linear gradients, both the $n = 1$ and $n = 2$ terms of Eq. 12 are present, the $n = 1$ term being due to the main field H_0 and the $n = 2$ term due to the gradient. The term corresponding to $n = 1$ rephases at all echoes as shown above. The $n = 2$ term after the first inversion ($j = 1$) becomes

$$\Phi_1^2 = \gamma^* g^* v/2^*(t^2 - 2^*\tau^2) \quad (16)$$

which, evaluated at the first echo ($t = 2^*\tau$), yields

$$\Phi_1^2 = g^* v^* \gamma /2\ (4^*\tau^2 - 2^*\tau^2) = g^*\gamma^* v^*\ \tau^2 \quad (17)$$

which is the classic expression for phase gain at the first echo derived by Hahn (3,4). On second echo ($j = 2$, $t = 4^*\tau$)

$$\Phi_2^2 = g^* v^*\gamma/2\ (t^2 - 16^*\tau^2)$$
$$= g^* v^*\gamma/2\ (16^*\tau^2 - 16^*\tau^2) = 0 \quad (18)$$

This result is true at all the even echoes, as the reader can easily verify using Table 1.

Equation 12 can be used to describe the degree of rephasing in any gradient. Terms higher than quadratic do not rephase at the early echoes. Thus, the degree of rephasing on even echoes during flow depends on the size of the quadratic term. Gradients that produce large quadratic terms in Eq. 12 will show strong rephasing on even echoes, whereas gradients producing small quadratic terms will not.

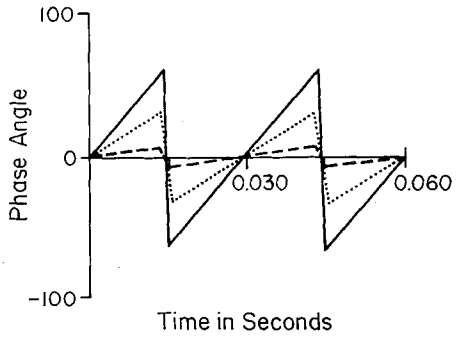

FIG. 2. Phase graph. Stationary isochromats in differing values of the magnetic field show 180° phase inversion at 15 and 45 ms. Complete rephasing appears at all echoes.

Figures 2–4 graphically demonstrate the above discussion. These figures were generated by direct numerical integration of the Larmor equation. In Figure 2 the phase lines correspond to stationary isochromats in different positions of the magnetic field. Due to the field gradient, the isochromats gain phase at different rates but rephase completely at all echoes. Figure 3 shows an example of isochromats that are initially at different values of the field and move through the linear gradient field at the same velocity. These isochromats do not rephase on the odd echoes but do rephase on the even echoes. Similarly, Fig. 4 shows the situation of a linear gradient and isochromats moving at different velocities. Initially the nine curves are grouped into three sets of three isochromats each. Within each set there are small velocity differences. As can be seen after the first echo, the phase dispersion is large with overlap developing between the isochromats of the various groups. Nevertheless, all isochromats continue to rephase at the even echoes.

Figures 5–8 were obtained with the Diasonics 0.35 T whole body NMR imager. Pulsing sequence was a spin echo with echoes at 28 and 56 ms and image reconstruction done by the two-dimensional

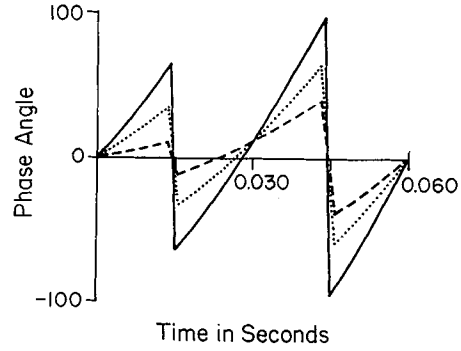

FIG. 3. Phase graph. All isochromats are at same velocity but at different positions in magnetic field. A magnetic field gradient exists in the direction of flow. There is incomplete rephasing at first echo and complete rephasing at second echo.

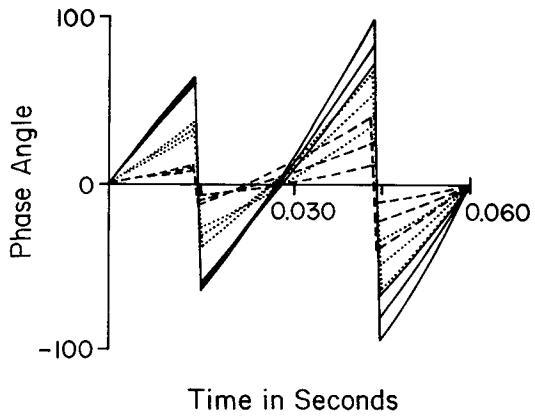

FIG. 4. Phase graph. Magnetic field gradient present in the direction of flow. Nine isochromats in groups of three with relative velocities of 1.0, 5.0, and 10.0. Within each group there is a small velocity dispersion. At the second phase inversion there is phase overlap among the groups. Complete rephasing is present only at the second echo.

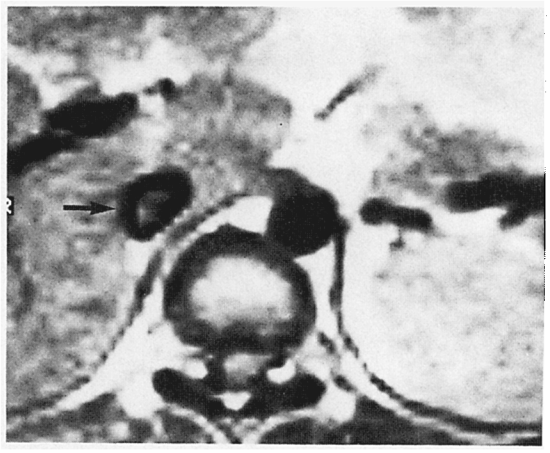

FIG. 5. Flow related enhancement in inferior vena cava. Typical increase in intensity is due to unsaturated protons entering the slice (arrow).

Fourier transform technique (7). Figure 5 shows typical flow related enhancement on the first echo in the inferior vena cava as blood first enters the imaging volume. Magnetic field gradients producing the rephasing are the plane selection and refocusing gradients. Figure 6 shows the hepatic and portal venous systems. There is no flow related enhancement on the first echo. However, on the second echo there is prominent enhancement of the venous system. The magnetic field gradients responsible for this effect are the readout gradients. Figure 7 shows this phenomenon in the transverse sinuses. In this case there is some flow related enhancement on the first echo in the upper figure with marked increase in intensity on second echo. Figure 8 shows additional clinical utility of the rephasing concept. In Fig. 8a there is a high intensity area in the right temporal bone. Without the second echo (Fig. 8b) this might possibly be misinterpreted as a pathological process such as a fat-containing lesion or epidermoid. However, on the second echo this can unambiguously be identified as flow in the sigmoid sinus and jugular bulb.

As can be seen from the above discussion, the

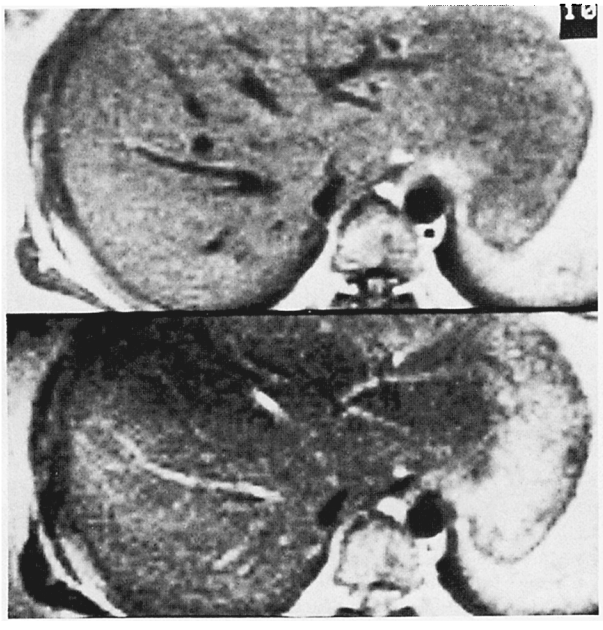

FIG. 6. Even echo rephasing. The magnetic field gradients present during readout are responsible for the prominent second echo rephasing of the hepatic venous system (bottom). No flow related enhancement is present on first echo (top).

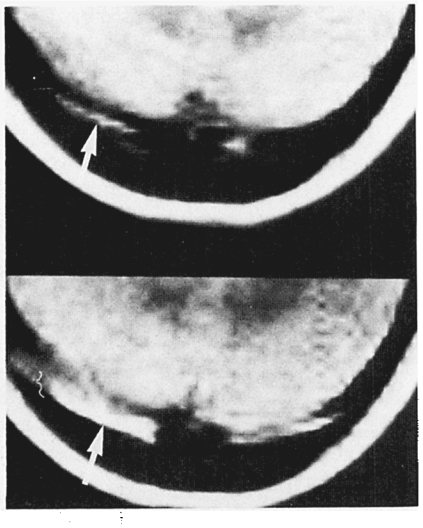

FIG. 7. Intensity enhancement due to combined flow effects. At first echo (top) there is increased intensity in the right transverse sinus (arrow) due to flow related enhancement. There is additional increase (bottom) in intensity (arrow) due to even echo rephasing.

8a,b

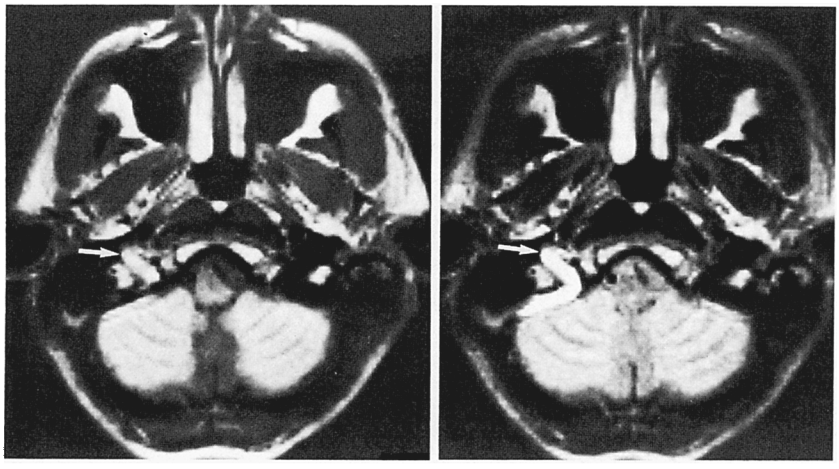

FIG. 8. Pseudotumor. High intensity structure in right temporal bone (arrow, **a**) may suggest a pathological process. Marked increase in intensity on second echo (arrow, **b**) indicates that the lesion is slow laminar flow in the sigmoid sinus and jugular bulb.

appearance of flow in the presence of magnetic field gradients can be quite complex. Although the concept of rephasing on even echoes has been known for many years (3–5), its appearance on NMR images has not been well appreciated in the NMR imaging literature. It has been included with "paradoxical enhancement" (8–11), a term originally coined to indicate flow related enhancement.

The appearance of flow on even and odd echoes, of course, depends on the particular type of pulsing sequence and gradient pulses used (12–15). In spin-echo sequences the intensity is also determined by the parameter TE. For longer TE more time is available for protons to leave the imaging volume and not contribute to the spin-echo signal emitted. At high flow velocities little rephasing occurs because of turbulence and high velocity signal loss. In addition, for a multislice acquisition sequence, retained saturation acquired from the upstream slices will affect the signal intensity in the downstream slices.

CONCLUSIONS

The general expressions for isochromat phase gain for fluids moving through magnetic field gradients have been derived. These expressions were applied in detail to the cases of flow and no flow in the presence and absence of a linear gradient. In the case of linear gradients in the presence of slow laminar flow, rephasing of isochromats was shown to occur on all even echoes and not on odd echoes. This resulted in second spin-echo signals having amplitudes greater than those of the first echo. Clinically this is seen as vessels appearing brighter on the second echo than on the first. This characteristic permits the identification of veins during clinical imaging. The phenomenon of flow related enhancement as seen on the first echo is unrelated to rephasing of isochromats, a phenomenon only seen on even numbered echoes.

REFERENCES

1. Bird RB, Stewart WE, Lightfoot EN. *Transport phenomena.* New York: John Wiley and Sons, 1960.
2. Bradley WG, Waluch V. NMR imaging of blood flow. Presented at the 69th Scientific Assembly and Annual Meeting of the Radiological Society of North America. *Radiology* 1983;149(p):28.
3. Hahn EL. Spin echoes. *Phys Rev* 1950;80:580–94.
4. Hahn EL. Detection of sea water motion by nuclear precession. *J Geophys Res* 1960;65:776–7.
5. Singer JR. NMR diffusion and flow measurements and an introduction to spin phase graphing. *J Phys* [*E*] 1978;11: 281–91.
6. Morse PM, Feshbach H. *Methods of theoretical physics.* New York: McGraw-Hill, 1953.
7. Crooks LE, Arakawa M, Hoenninger J, et al. Nuclear magnetic resonance whole body imager operating at 3.5K gauss. *Radiology* 1982;143:169–81.
8. Crooks L, Mills CM, Davis PL, et al. Visualization of cerebral and vascular abnormalities by NMR imaging–the effects of imaging parameters on contrast. *Radiology* 1982;144:843–52.
9. Herfkens RJ, Higgins CB, Hricak H, et al. Nuclear magnetic resonance imaging of atherosclerotic disease. *Radiology* 1983;148:161–6.
10. Herfkens RJ, Higgins CB, Hricak H, et al. Nuclear magnetic resonance imaging of the cardiovascular system: normal and pathological findings. *Radiology* 1983;147:749–58.
11. Crooks L, Sheldon P, Kaufman L, Rowan W. Quantification of obstructions in vessels by nuclear magnetic resonance in NMR. *IEEE Trans Nucl Sci* 1982;NS-29:1181–5.
12. Singer JR. Blood flow rates by nuclear magnetic resonance measurements. *Science* 1959;130:1652–3.
13. Singer JR. Blood flow imaging by NMR. In: Kaufman L, Crooks LE, Margulis AR, eds. *Nuclear magnetic imaging in medicine.* New York: Igaku-Shoin, 1981;128–44.
14. Mansfield P, Morris PG. *NMR imaging in biomedicine.* New York: Academic Press, 1982.
15. Singer JR. Blood flow measurements by NMR of the intact body. In: Partain CL, James AE, Rollo FD, Price RR, eds. *Nuclear magnetic resonance (NMR) imaging.* Philadelphia: WB Saunders, 1983:168–78.